An Improved Phenomenological Model for Polymer Desorption

Joanna Sooknanan and Donna Comissiong

Abstract—We propose a phenomenological model for the process of polymer desorption. In so doing, we omit the usual theoretical approach of incorporating a fictitious viscoelastic stress term into the flux equation. As a result, we obtain a model that captures the essence of the phenomenon of trapping skinning, while preserving the integrity of the experimentally verified Fickian law for diffusion. An appropriate asymptotic analysis is carried out, and a parameter is introduced to represent the speed of the desorption front. Numerical simulations are performed to illustrate the desorption dynamics of the model. Recommendations are made for future modifications of the model, and provisions are made for the inclusion of experimentally determined frontal speeds.

Index Terms—Phenomenological Model, Polymer, Desorption, Trapping Skinning

I. INTRODUCTION

The study of polymers and their properties has been a key area of investigation for experimentalists and theorists in recent years. Material scientists are continually seeking to capitalize on the designer qualities inherent in polymers. Novel polymeric blends have proven advantageous for the pharmaceutical, clothing and sealant industries. In order to make accurate predictions for the industrial use of polymers, there is a definite need for accurate mathematical models for polymeric behavior. Owing to the complexity of the behavior of polymeric materials, the mathematical modeling of such systems is particularly challenging.

When a penetrant diffuses into a dry crosslinked polymeric network (i.e. polymer sorption), its molecules assume new configurations in an attempt to accommodate incoming penetrant molecules. This triggers a swelling process, which transforms the polymer to a saturated "swelled"state. In contrast, a polymer already in its saturated "swelled"state has the potential to lose solvent to its surroundings (i.e. polymer desorption). As expected, this loss of solvent triggers the reverse change of state in the polymer, which subsequently resumes a semblance of its original dry configuration. We note that the desorption process is not an exact reversal of sorption. We remark that this is an overly simplified mode of describing a complicated mechanical process, owing to the nonlinear structure of polymeric chains. We do not take kinetic or thermo-mechanical effects into consideration. In the absence of experimental data, we base in our model on the experimentally verified equations governing diffusion.

J. Sooknanan and D. M. G. Comissiong are with the Department of Mathematics and Computer Science, The University of the West Indies, St. Augustine, Trinidad and Tobago e-mail: Donna.Comissiong@sta.uwi.edu
Manuscript received March 10th, 2009

However, in the face of such complexity, any simplified model is a step towards attaining a better understanding of the process, and is worthy of attention. It is a known fact that penetrant transport in complex materials, such as polymers, often deviates from the predictions of Fick's law. Several anomalies associated with mass uptake have been documented in polymer sorption experiments [1]. Such features are often termed anomalous or simply as non-Fickian.

Several attempts have been made to develop mathematical models for anomalous diffusion in polymers. For anomalous sorption, two main approaches are commonly utilized. The first class of models are based on Fick's law while attempting to incorporate features of the experimentaily documented glass-rubber polymer transition kinetics (see e.g. [2], [3], [4], [5], [6], [7], [8], [9], [10], [11]). Such phenomenological formulations tend to be preferred by experimental polymer scientists. In the second approach, Fick's law is modified by incorporating a viscoelastic stress term into the flux equation. A variant of the linear Maxwell viscoelastic model is often adopted to define a polymer stress relaxation time. This parameter is then utilized to account for glass-rubber transition dynamics in the swelling polymer (see e.g. [12],[13]). This more theoretical approach has been adopted mainly by applied mathematicians. For simplicity, and for comparison with the existing models for polymer desorption to-date (see e.g. [14], [15]), we will refer to the swelled saturated state as "rubbery", and the unswelled polymer state as "glassy". The reader should not however, that this is not a literal description of the process at hand, and by no means should be interpreted as a pysical phase change from a brittle glassy state to a flexible rubbery state.

Much less attention has been given to the mathematical modeling of polymer desorption. This could be a direct result of the fact that experimental values for the velocity of the rubber-glass transition front are not readily available in the literature. Indeed, it is difficult to obtain such measurements as a result of the complicated process of crystallization, which inhibits the experimental probes utilized to measure transition front speed. It should be pointed out that desorption is not a simple reversal of the related sorption process. Anomalous behavior is less varied and not easily detectable in the case of polymer desorption. Experimental results often portray a remarkable resemblance between desorption dynamics and Fickian diffusive traits. It has also been verified that polymer desorption is much faster than polymer sorption [16].

Owing to the absence of experimental data, it is difficult to conceive a phenomenological model to describe polymer desorption. As a result, most mathematical models developed

to-date adopt a more theoretical approach by incorporating a viscoelastic stress term into the flux equation, as done previously for Case II polymer diffusion (see e.g. [14], [15]). Numerical simulations obtained for polymer desorption models that utilize this approach at times exhibit sharp separation fronts. We remark that this feature is discordant with the experimental data presented in [1] and [16].

In this paper, we propose a phenomenological model for polymer desorption based on Fick's law, and a rate controlled motion of the moving front separating the glassy and rubbery regions. A simpler version of this model has been recently conceived by Comissiong *et al.* [17]. In the absence of a standard expression for the speed of desorption front, we consider concentrations for the glassy and rubbery states that depend on a certain parameter. This parameter may be specified once a particular expression for the frontal speed becomes available. Therefore, our model provides a viable starting point for future experimental studies on polymer desorption, as an appropriate velocity expression can be easily incorporated.

The paper is organized as follows. A description of the derived model is first presented. The analysis is based on a pair of coupled partial differential equations together with a moving, approximately Fickian boundary that separates the glassy and rubbery regions. In light of experimental observations [18], this is not an unreasonable approximation. Since the system is not solvable by similarity solutions, an integral method developed by Boley is used to obtain asymptotic solutions. A preliminary test of validity of the proposed model is implemented by determining whether the model exhibits the traits of the experimentally documented trapping skinning effect. This is done by considering the relationship between accumulated flux and the force driving desorption. In our numerical simulations, changes in external concentration and permeability of the exposed end are utilized to modify the driving force. For trapping skinning we would expect a decrease in external concentration and an increase in permeability to decrease the accumulated flux. This trend is observed numerically with our polymer desorption model. The underlying assumptions inherent in the model are duly addressed. Numerical simulations illustrating polymer desorption dynamics are included. Finally, recommendations were given to improve this model via boundary layer theory and matched asymptotic expansions.

II. Governing Equations

Initially the polymer is saturated with concentration C_{init}. The concentration of the external environment is denoted by C_{ext} where for desorption to occur $C_{ext} < C_{init}$. The characteristic solute concentration that distinguishes the glassy from the swollen state is denoted by C_*. In the dry-glassy state the penetrant concentration C^g is such that $C^g < C_*$. In the saturated state the penetrant concentration C^r is such that $C^r > C_*$. The front position is denoted by $s(t)$.

Fick's law of diffusion is given by

$$J = -D(C)C_x,\qquad(1)$$

where $J = $ mass flux, $D(C) = $ molecular diffusion coefficient, $C = $ concentration, $x = $ distance from boundary through which solvent is free to move. Here and elsewhere, the subscript x refers to a partial derivative with respect to the variable x. There is a significant change in $D(C)$ as the polymer loses its solute and is transformed from the rubbery to the glassy state [19].

To obtain a system amenable to asymptotic techniques $D(C)$ is taken to be piecewise constant. We note that this is a widely accepted approximation in several models for diffusion in polymers (see e.g. [14], [13], [15] and the cited references). It is justified by the fact that differences within states are negligible when compared with the difference between states. Hence $D(C)$ is modelled by taking an average over each phase

$$D(C) = \begin{cases} D_g, \ 0 \le C \le C_*(glassy) \\ \\ D_r, \ C_* < C(rubbery) \end{cases}.\qquad(2)$$

Combining (1) with the standard conservation law

$$C_t = -J_x,\qquad(3)$$

where the time is represented by t, we obtain the partial differential equation for the concentration C

$$C_t = (D(C)C_x)_x.\qquad(4)$$

The form of (2) the physical system is modeled as a two-state problem with a moving boundary $x = s(t)$ representing the glass-rubber interface. Hence

$$C_t = \begin{cases} C_t^g = D_g C_{xx}^g, \ x < s(t) \\ \\ C_t^r = D_r C_{xx}^r, \ x \ge s(t) \end{cases}\qquad(5)$$

The boundary condition at the front is given by

$$C^r(s(t),t) = C_*, t > 0\qquad(6)$$

and the initial concentration is

$$C(x,0) = C_{init}, x > 0.\qquad(7)$$

The insulated far end is represented by

$$J(\infty,t) = 0, \ t \ge 0.\qquad(8)$$

At $x = 0$, we use

$$J(0,t) = K[C_{ext} - C(0,t)],\qquad(9)$$

where K is a constant measuring the permeability of the exposed boundary.

Using Fick's Law we have

$$-D(C)C_x(0,t) = K[C_{ext} - C(0,t)],\qquad(10)$$

which is the same as

$$C_x(0,t) = k[C(0,t) - C_{ext}],\qquad(11)$$

where $k = \dfrac{K}{D} > 0$. Upon solving the equation

$$\frac{\partial C(0,t)}{C(0,t) - C_{ext}} = k\partial x, \tag{12}$$

we obtain

$$C(0,t) = C_{ext} + m(t)e^{kx}, \tag{13}$$

where $m(t) > 0$ for all $t > 0$.

III. CONDITIONS ON $m(t)$

Since

$$C(0,0) = C_{init} \ , \tag{14}$$

this implies that

$$C(0,0) \quad = C_{ext} + m(0). \tag{15}$$

This means that

$$m(0)e^{kx} = C_{init} - C_{ext}. \tag{16}$$

As

$$C_{init} > C_{ext}, \ e^{kx} > 0, \tag{17}$$

it follows that

$$m(0) > 0. \tag{18}$$

Now consider the case $t \longrightarrow \infty$. Since

$$\underset{t \longrightarrow \infty}{Lim} C(0,t) \quad = C_{ext}, \tag{19}$$

taking limits as $t \longrightarrow \infty$ of (13) we obtain

$$C_{ext} = C_{ext} + \underset{t \longrightarrow \infty}{Lim} m(t)e^{kx}, \tag{20}$$

and it follows that

$$\underset{t \longrightarrow \infty}{Lim} m(t)e^{kx} = 0. \tag{21}$$

Also since $e^{kx} > 0$, we conclude that

$$\underset{t \longrightarrow \infty}{Lim} m(t) = 0 \tag{22}$$

IV. SPEED OF THE FRONT

As the flux J and the solute concentration C are discontinuous across the front, the frontal speed is defined by

$$s'(t)[C]_{s(t)} = [J]_{s(t)}. \tag{23}$$

Here $[h]_{s(t)} = h(s(t)_+, t) - h(s(t)_-, t)$ represents the jump of h at $s(t)$.

A. Small Time Behaviour

We now study the speed of the front by re-defining expressions for the concentration in the glassy and rubbery states in terms of fictitious initial and boundary conditions. These are then solved using an integral method originally developed by Boyle for standard diffusion problems and adopted by Edwards [20] for use in his polymer desorption models. The method is described as follows using the glassy region. The rubbery region will follow an analogous procedure.

It is assumed that $C_t^g = D_g C_{xx}^g$, $x < s(t)$, holds for the related function $T^g(x,t)$ in the entire semi-infinite domain $x > 0$. This function $T^g(x,t)$ is assumed to satisfy an unknown fictitious initial condition $f^i(x)$. It is also required to satisfy the relevant model equations. This related function, when restricted to $x < s(t)$, gives the required solution for $C^g(x,t)$ [20].

B. Glassy Concentration

The diffusion equation $C_t^g = D_g C_{xx}^g$, $x < s(t)$ is assumed to hold in the semi-infinite domain for some fictitious initial boundary condition at $x = 0$, $f^i(x)$. This condition is fictitious because the polymer is not glassy at $t = 0$. (Recall that the polymer is initially saturated.) The solution of this partial differential equation must satisfy condition (23), (7) and (8).

Let

$$C^g(x,t) = C(0,t) + T^g(x,t), \quad 0 < x < s(t), \tag{24}$$

which is the same as

$$C^g(x,t) = C_{ext} + m(t)e^{kx} + T^g(x,t) \tag{25}$$

for $0 < x < s(t)$. Here, T^g is defined by

$$\begin{cases} T_t^g = D_g T_{xx}^g, \ x > 0, t > 0 \\ T^g(0,t) = 0, \ t > 0 \\ T_x^g(\infty, t) = 0, \ t > 0 \\ T^g(x,0) = f^i(x), x > 0 \end{cases} . \tag{26}$$

The solution of (26) is given by [21] to be

$$T^g(x,t) = \frac{1}{\sqrt{4\pi D_g t}} \int_0^\infty f^i(y) \left(\begin{array}{c} e^{-\frac{(x-y)^2}{4D_g t}} \\ -e^{-\frac{(x+y)^2}{4D_g t}} \end{array} \right) dy, \tag{27}$$

where

$$C^g(x,t) = C_{ext} + m(t)e^{kx} +$$
$$\frac{1}{\sqrt{4\pi D_g t}} \int_0^\infty f^i(y) \left(\begin{array}{c} e^{-\frac{(x-y)^2}{4D_g t}} - \\ e^{-\frac{(x+y)^2}{4D_g t}} \end{array} \right) dy, \tag{28}$$

for $0 < x < s(t)$.

C. Rubbery Concentration

The diffusion equation $C_t^r = D_r C_{xx}^r$, $x > s(t)$ is assumed to hold in the semi-infinite domain for some fictitious Dirichlet boundary condition at $x = 0$, $f_b(t)$. This condition is fictitious because the rubbery part occupies the region $s(t) < x < \infty$. The solution of this partial differential equation must satisfy condition (6), (23), (7) and (8).

We consider

$$C^r(x,t) = C_{init} - T^r(x,t), \ x > s(t). \quad (29)$$

Here, T^r is defined by

$$\begin{cases} T_t^r = D_r T_{xx}^r, \ x > 0, t > 0 \\ T^r(0,t) = f_b(t), \ t > 0 \\ T_x^r(\infty,t) = 0, \ t > 0 \\ T^r(x,0) = 0, x > 0 \end{cases}. \quad (30)$$

The solution of (30) is given by [21]

$$T^r(x,t) = f_b(t) + \int_0^t \frac{1}{\sqrt{4\pi(t-\tau)}} *$$
$$\left[\int_0^\infty -f_b'(\tau)(e^{-\frac{(x-y)^2}{4D_r(t-\tau)}} - e^{-\frac{(x+y)^2}{4D_r(t-\tau)}}) dy \right] d\tau. \quad (31)$$

The second integral on the right hand side of the equation can be expressed as

$$\int_0^t \frac{\left(\int_0^\infty -f_b'(\tau) \left(\begin{array}{c} e^{-\frac{(x-y)^2}{4D_r(t-\tau)}} \\ -e^{-\frac{(x+y)^2}{4D_r(t-\tau)}} \end{array} \right) dy \right)}{\sqrt{4\pi D_r(t-\tau)}} d\tau$$
$$= -f_b(t) + \frac{x}{\sqrt{4\pi D_r}} \int_0^t \frac{f_b(\tau)e^{-\frac{x^2}{4D_r(t-\tau)}}}{(t-\tau)^{3/2}} d\tau. \quad (32)$$

This leads to

$$C^r(x,t) = C_{init} -$$
$$\frac{x}{\sqrt{4\pi D_r}} \int_0^t \frac{f_b(\tau)e^{-\frac{x^2}{4D_r(t-\tau)}}}{(t-\tau)^{3/2}} d\tau \quad (33)$$

for $x > s(t)$

D. The Fictitious initial and boundary terms f^i and f_b

1) Small time behavior: $t \to 0$: From [20], the following forms are assumed.

$$f^i(x) = f_0^i, \quad f_b(t) = f_0^b, \quad s(t) = 2s_0 t^n. \quad (34)$$

where f_0^i, f_0^b and n are to be determined. Using (34) and properties of $erfc$, the concentration in the rubbery state (33) is found to be:

$$C^r(x,t) = C_{init} -$$
$$\frac{x}{\sqrt{4\pi D_r}} \int_0^t \frac{f_0^b e^{-\frac{x^2}{4D_r(t-\tau)}}}{(t-\tau)^{3/2}} d\tau \quad (35)$$

for $x > s(t)$. This is simplified to

$$C^r(x,t) = C_{init} -$$
$$\frac{xf_0^b}{\sqrt{4\pi D_r}} \int_0^t \frac{\exp\left(-\frac{x^2}{4D_r(t-\tau)}\right)}{(t-\tau)^{3/2}} d\tau \quad (36)$$

This can be written in a more elegant form in terms of the error function if we let

$$z = \sqrt{\frac{x^2}{4D_r(t-\tau)}}, \quad (37)$$

then

$$dz = \frac{1}{2}\sqrt{\frac{x^2}{4D_r}}(t-\tau)^{\frac{-3}{2}} d\tau$$
$$\implies (t-\tau)^{\frac{-3}{2}} d\tau = \frac{4}{x}\sqrt{D_r} dz. \quad (38)$$

We note that for the case $\tau = 0$,

$$z = \sqrt{\frac{x^2}{4D_r t}}. \quad (39)$$

Now consider

$$\tau = t \implies z = \infty. \quad (40)$$

Substituting this into (36) we have

$$C^r(x,t) = C_{init} - \frac{4xf_0^b \sqrt{D_r}}{x\sqrt{4\pi D_r}} \int_{\sqrt{\frac{x^2}{4D_r t}}}^\infty e^{-z^2} dz. \quad (41)$$

Writing this in terms of the error function, we obtain

$$C^r(x,t) = C_{init} - f_0^b erfc(\frac{x}{\sqrt{4D_r t}}). \quad (42)$$

Next, (6) allows us to express C^r at the front as

$$C_* = C^r(s(t),t)$$
$$= C_{init} - f_0^b erfc\frac{s_0 t^{n-\frac{1}{2}}}{\sqrt{D_r}}. \quad (43)$$

For $n < \frac{1}{2}$, $C^r(s(t),t) \to C_{init}$, when $t \to 0$, this would imply $C_{init} = C_*$. This is impossible as $C_{init} > C_*$ as the polymer is initially saturated. Hence it follows that

$$n \geq \frac{1}{2} \text{ for small time behavior.} \quad (44)$$

Using (34) and properties of $erfc$, the concentration in the glassy state (28) is simplified to give

$$C^g(x,t) = C_{ext} + m(t)e^{kx} + \frac{f_0^i}{\sqrt{\pi}} \int_{-\frac{x}{\sqrt{4D_g t}}}^{\frac{x}{\sqrt{4D_g t}}} e^{-z^2} \, dz,$$

This may be expressed in terms of the error function as

$$C^g(x,t) = C_{ext} + m(t)e^{kx} + f_0^i erf\frac{x}{\sqrt{4D_g t}} \qquad (45)$$

for $0 < x < s(t)$. At the front $s(t)$, C^g is given by

$$C^g(s(t)_-, t) = C_{ext} + m(t)e^{kx} + f_0^i erf\frac{s_o t^{n-\frac{1}{2}}}{\sqrt{D_g}}. \qquad (46)$$

However, since (44) $n \geq \frac{1}{2}$ as $t \to 0$, for small time, it was deduced that

$$C^g(s(t)_-, t) \to C_{ext} + m(0)e^{kx} \qquad (47)$$

At this point, there is sufficient information to justify (23) which claims that the concentration is discontinuous at the front.

We now prove that $C(x,t)$ is discontinuous at the front using the method of contradiction. Let us assume that C is continuous at the front. Then

$$C^g(s(t)_-, t) = C^r(s(t), t) = C_* \qquad (48)$$

and

$$C_{ext} + m(0)e^{kx} = C_*. \qquad (49)$$

Therefore

$$C_{ext} + C_{init} - C_{ext} = C_*, \qquad (50)$$

and this implies that

$$C_{init} = C_*. \qquad (51)$$

This is impossible as $C_{init} > C_*$. Hence $C(x,t)$ is not continuous.

Therefore we are justified in our choice of a discontinuity of front concentration. This lack of continuity gives the desorption front in our model a measure of non-Fickian character. It is note mentioning that the desorption models of Edwards [20] assume continuous front concentration.

2) Large time behavior: $t \to \infty$: From [20], the following

forms are assumed:

$$f^i(x) = f_\infty^i e^{Ax}, \; f_b(t) = f_\infty^b e^{B^2 t}, \; s(t) = 2s_\infty t^n, \qquad (52)$$

where f_∞^i, f_∞^b, A, B and n are to be found. Using the above and properties of erf, the concentration in the glassy state (28) may be simplified to

$$C^g(x,t) = C_{ext} + m(t)e^{kx}$$
$$+ \frac{f_\infty^i e^{A^2 D_g t}}{\sqrt{\pi}} \left(\begin{array}{l} e^{Ax} \int_{-\frac{x+2AD_g t}{\sqrt{4D_g t}}}^{\infty} e^{-z^2} \, dz \\ -e^{-Ax} \int_{\frac{x-2AD_g t}{\sqrt{4D_g t}}}^{\infty} e^{-z^2} \, dz \end{array} \right). \qquad (53)$$

Employing the $erfc$ function, this can be rewritten as

$$C^g(x,t) = C_{ext} + m(t)e^{kx}$$
$$+ \frac{f_\infty^i}{2} e^{A^2 D_g t} \left[\begin{array}{l} e^{Ax} \operatorname{erf} c\left(-\frac{x+2AD_g t}{\sqrt{4D_g t}}\right) \\ - e^{-Ax} \operatorname{erf} c\left(\frac{x-2AD_g t}{\sqrt{4D_g t}}\right) \end{array} \right] \qquad (54)$$

for $0 < x < s(t)$.

A can be determined by taking the limit of (54) as $t \to \infty$. Using $\operatorname{erf} c(-w) = 2 - \operatorname{erf} c(w)$, C^g can be written as

$$C^g(x,t) = C_{ext} + m(t)e^{kx}$$
$$+ \frac{f_\infty^i}{2} \left[\begin{array}{l} 2e^{A^2 D_g t}(e^{Ax} - e^{-Ax}) \\ +e^{-Ax+A^2 D_g t} \operatorname{erf} c\left(\frac{-x+2AD_g t}{\sqrt{4D_g t}}\right) \\ - e^{Ax+A^2 D_g t} \operatorname{erf} c\left(\frac{x+2AD_g t}{\sqrt{4D_g t}}\right) \end{array} \right]. \qquad (55)$$

We note that

$$\lim_{t\to\infty} e^{\frac{\gamma x + \gamma^2 t}{\alpha^2}} \operatorname{erf} c\left(\frac{x+2\gamma t}{2\alpha\sqrt{t}}\right) =$$
$$\lim_{t\to\infty} \frac{2\alpha\sqrt{t}}{\sqrt{\pi}(x+2\gamma t)} e^{-\frac{x^2}{4\alpha^2 t}}. \qquad (56)$$

On taking large time limits, the $erfc$ terms in (55) can be simplfied as follows

$$\lim_{t\to\infty} e^{-Ax+A^2 D_g t} \operatorname{erf} c\left(\frac{-x+2AD_g t}{\sqrt{4D_g t}}\right) =$$
$$\lim_{t\to\infty} \frac{2\sqrt{D_g t}}{\sqrt{\pi}(-x+2AD_g t)} e^{-\frac{x^2}{4D_g t}}. \qquad (57)$$

Also

$$\lim_{t\to\infty} e^{Ax+A^2 D_g t} \operatorname{erf} c\left(\frac{x+2AD_g t}{\sqrt{4D_g t}}\right) =$$
$$\lim_{t\to\infty} \frac{2\sqrt{D_g t}}{\sqrt{\pi}(x+2AD_g t)} e^{-\frac{x^2}{4D_g t}}. \qquad (58)$$

Finally, using $\lim_{t\to\infty} m(t) = 0$, (55) reduces to

$$\lim_{t\to\infty} C^g(x,t) = \lim_{t\to\infty} \left[f_\infty^i \left(\begin{array}{l} C_{ext} + \\ e^{A^2 D_g t}(e^{Ax} - e^{-Ax}) \\ +e^{-\frac{x^2}{4D_g t}}\left(\frac{\sqrt{D_g t}}{\sqrt{\pi}(-x+2AD_g t)}\right. \\ \left. -\frac{\sqrt{D_g t}}{\sqrt{\pi}(x+2AD_g t)}\right) \end{array} \right) \right]. \qquad (59)$$

The limit in the above is finite provided that $A = 0$. For the case where $A = 0$, (54) becomes

$$C^g(x,t) = C_{ext} + m(t)e^{kx} + \frac{f^i_\infty}{2}\left[\begin{array}{c} \mathrm{erf}\,c\left(-\dfrac{x}{\sqrt{4D_g t}}\right) \\ -\,\mathrm{erf}\,c\left(\dfrac{x}{\sqrt{4D_g t}}\right) \end{array}\right].$$
(60)

Using the identities $erfc(z) = 1 - erf(z)$ and $erfc(-z) = -erf(z)$, it follows that

$$C^g(x,t) = C_{ext} + m(t)e^{kx} + f^i_\infty \mathrm{erf}\left(\frac{x}{\sqrt{4D_g t}}\right)$$
(61)

and $A = 0$.

B can be determined by considering the concentration in the rubbery state. Substituting $f_b(t) = f^b_\infty e^{B^2 t}$ into (33), we obtain for $x \geqslant s(t)$

$$C^r(x,t) = C_{init} -$$

$$\frac{f^b_\infty e^{B^2 t}}{2}\left[\begin{array}{c} e^{\frac{Bx}{\sqrt{D_r}}}erfc\left(\dfrac{x + 2Bt\sqrt{D_r}}{\sqrt{4D_r t}}\right) \\ +e^{-\frac{Bx}{\sqrt{D_r}}}erfc\left(\dfrac{x - 2Bt\sqrt{D_r}}{\sqrt{4D_r t}}\right) \end{array}\right],$$
(62)

From (56) we have

$$\lim_{t\to\infty} e^{B^2 t + \frac{Bx}{\sqrt{D_r}}}erfc\left(\frac{x + 2Bt\sqrt{D_r}}{\sqrt{4D_r t}}\right) =$$
$$\lim_{t\to\infty} \frac{2\sqrt{D_r}\,t}{\sqrt{\pi}(x + 2Bt\sqrt{D_r}\,)}e^{-\frac{x^2}{4Dr\,t}}.$$
(63)

Substituting this into the large-time limit of (62), we obtain for $x \geqslant s(t)$

$$\lim_{t\to\infty} C^r(x,t) = C_{init} -$$

$$\frac{f^b_\infty}{2}\left[\begin{array}{c} \lim\limits_{t\to\infty} e^{-\frac{x^2}{4Dr\,t}}\dfrac{2\sqrt{D_r}\,t}{\sqrt{\pi}(x+2Bt\sqrt{D_r}\,)} \\ +\lim\limits_{t\to\infty} e^{B^2 t - \frac{Bx}{\sqrt{D_r}}}\mathrm{erf}\,c\left(\dfrac{x - 2Bt\sqrt{D_r}}{\sqrt{4D_r t}}\right) \end{array}\right].$$
(64)

Now

$$\lim_{t\to\infty} e^{-\frac{x^2}{4Dr\,t}}\frac{2\sqrt{D_r}\,t}{\sqrt{\pi}(x+2Bt\sqrt{D_r}\,)} = 0,$$
(65)

so for $\lim\limits_{t\to\infty} C^r(x,t)$ to be bounded, either

$$B = 0,$$
(66)

or

$$B^2 t - \frac{Bx}{\sqrt{D_r}} < 0, \quad \text{i.e.} \quad x \geqslant \sqrt{D_r}Bt,$$
(67)

and this is valid in the region $x \geqslant s(t)$ (where $s(t) = \sqrt{D_r}Bt$). These two cases are now examined.

3) CASE 1: $B = 0$: When $B = 0$, (62) becomes

$$C^r(x,t) = C_{init} - \frac{f^b_\infty}{2}\left(\begin{array}{c} erfc\left(\dfrac{x}{\sqrt{4D_r t}}\right) \\ +erfc\left(\dfrac{x}{\sqrt{4D_r t}}\right) \end{array}\right),$$
(68)

which is equivalent to

$$C^r(x,t) = C_{init} - f^b_\infty erfc\left(\frac{x}{\sqrt{4D_r t}}\right).$$
(69)

The large-time concentrations C^g and C^r are now analysed at the front $s(t)$. Substituting $s(t)$ into (69) gives

$$C^r(s(t),t) = C_{init} - f^b_\infty erfc\left(\frac{s_\infty t^{n-\frac{1}{2}}}{\sqrt{D_r}}\right).$$
(70)

It follows that for $n > \frac{1}{2}$ and $t \to \infty$, $C^r(s(t),t) \to C_{init}$. As $C^r(s(t),t) = C_*$, this would imply that $C_* = C_{init}$. This is not possible as $C_* < C_{init}$. Hence we may conclude that

$$n \leq \frac{1}{2}$$
(71)

for large time behavior when $B = 0$.

4) Case 2: $s(t) = \sqrt{D_r}Bt$: Utilizing (6) where $C^r(s(t),t) = C_*$ in (62) gives

$$C^r(s(t),t) = C_{init} -$$

$$\frac{f^b_\infty}{2}e^{B^2 t}\left[\begin{array}{c} e^{B\frac{\sqrt{D_r}Bt}{\sqrt{D_r}}}\mathrm{erf}\,c\left(\dfrac{Bt\sqrt{D_r} + 2Bt\sqrt{D_r}}{\sqrt{4D_r t}}\right) \\ +e^{-B\frac{\sqrt{D_r}Bt}{\sqrt{D_r}}}\mathrm{erf}\,c\left(\dfrac{Bt\sqrt{D_r} - 2Bt\sqrt{D_r}}{\sqrt{4D_r t}}\right) \end{array}\right],$$
(72)

which on simplifying gives

$$C^r(s(t),t) = C_{init} -$$

$$\frac{f^b_\infty}{2}e^{B^2 t}\left[\begin{array}{c} e^{B\frac{\sqrt{D_r}Bt}{\sqrt{D_r}}}\mathrm{erf}\,c\left(\dfrac{3Bt\sqrt{D_r}}{\sqrt{4D_r t}}\right) \\ +e^{-B\frac{\sqrt{D_r}Bt}{\sqrt{D_r}}}\mathrm{erf}\,c\left(\dfrac{-Bt\sqrt{D_r}}{\sqrt{4D_r t}}\right) \end{array}\right].$$
(73)

Now taking $t \to \infty$, we obtain

$$C^r(s(t),t) = C_{init} - \frac{f^b_\infty}{2}\left[erfc\left(\frac{-Bt\sqrt{D_r}}{\sqrt{4D_r t}}\right)\right].$$
(74)

Since $erfc(-\infty) = 2$, as $t \to \infty$ we have

$$C^r(s(t),t) = C_{init} - f^b_\infty = C_*.$$
(75)

Using the expressions for $C^r(s(t),t)$, $C^g(s(t)_-,t)$ to determine expressions for $C^r_x(s(t),t)$ and $C^g_x(s(t)_-,t)$, taking limits as $t \to \infty$ and substituting in (23), we now determine the validity of the expression for front position $s(t) = \sqrt{D_r}Bt$.

From (61)

$$C^g(x,t) = C_{ext} + m(t)e^{kx} + f^i_\infty \text{erf}\left(\frac{x}{\sqrt{4D_g t}}\right). \qquad (76)$$

Substituting

$$x = s(t) = \sqrt{D_r} Bt \qquad (77)$$

and taking limits as $t \to \infty$, we obtain

$$C^g(s(t)_-, t) = C_{ext} + f^i_\infty. \qquad (78)$$

The derivation of $C^g_x(s(t)_-, t)$ is as follows:

$$C^g(x,t) = C_{ext} + m(t)e^{kx} + f^i_\infty \text{erf}\left(\frac{x}{\sqrt{4D_g t}}\right). \qquad (79)$$

Differentiating with respect to x yeilds,

$$C^g_x = f^i_\infty \frac{2}{\sqrt{\pi}} e^{-\frac{x^2}{4D_g t}} \left(\frac{1}{\sqrt{4D_g t}}\right) + km(t)e^{kx}, \qquad (80)$$

Substituting for $s(t)$ and taking large time limits gives

$$C^g_x(s(t),t) = 0. \qquad (81)$$

The partial differential of C^r with respect to x follows a similar proceedure. After substituting for $s(t)$, we get

$$C^r_x(s(t),t) = f^b_\infty \frac{B}{\sqrt{D_r}}. \qquad (82)$$

Utilizing (75) in the above yields

$$C^r_x = (C_{init} - C_*) \frac{B}{\sqrt{D_r}}, \qquad (83)$$

The expressions for $C^r(s(t),t), C^g(s(t)_-,t), \ C^r_x(s(t),t),$ $C^g_x(s(t)_-,t)$, and (6) are substituted into (23) to obtain

$$s' \{C^r(s(t)_+,t) - C^g(s(t)_-,t)\} = $$
$$D_g C^g_x(s(t)_-,t) - D_r C^r_x(s(t),t). \qquad (84)$$

Substituting for $C^r(s(t),t), C^g(s(t)_-,t), \ C^r_x(s(t),t),$ $C^g_x(s(t)_-,t)$ and s' we obtain

$$\sqrt{D_r} B \{C_* - C_{ext} - f^i_\infty\} = -\frac{D_r(C_{init} - C_*)B}{\sqrt{D_r}}. \qquad (85)$$

This implies that

$$f^i_\infty = C_{init} - C_{ext}. \qquad (86)$$

Using this expression in (61) and taking limits as $t \to \infty$ and $s(t) = \sqrt{D_r} Bt$ gives

$$\lim_{t\to\infty} C^g(s(t)_-,t) = C_{ext} + f^i_\infty \lim_{t\to\infty} \text{erf}\left(\frac{\sqrt{D_r}Bt}{2\sqrt{D_g t}}\right), \qquad (87)$$

which on simplification leads to

$$\lim_{t\to\infty} C^g(s(t)_-,t) = C_{ext} + f^i_\infty. \qquad (88)$$

On substituting for f^i_∞ this reduces to

$$\lim_{t\to\infty} C^g(s(t)_-,t) = C_{ext} + C_{init} - C_{ext}, \qquad (89)$$

which means that

$$\lim_{t\to\infty} C^g(s(t)_-,t) = C_{init}. \qquad (90)$$

This allows us to conclude that $C_{init} < C_*$. However this is not true as for desorption $C_{init} > C_*$ (as the polymer is initially saturated). Clearly, this second case is unrealistic. Hence $B = 0$ and $n \leqslant \frac{1}{2}$. It follows that the speed of the front behaves like

$$t^{n-1} = \begin{cases} n \geqslant \frac{1}{2} & t \to 0 \\ n \leqslant \frac{1}{2} & t \to \infty \end{cases} \qquad (91)$$

V. Dependence of the Moving Front on Problem Data

We now analyse the behavoir of the moving front when $n = \frac{1}{2}$. This choice for n has been justified previously.

5) Small time behavior: From (34) the expression for the front position $s(t)$ becomes

$$s(t) = 2s_0\sqrt{t}. \qquad (92)$$

Substituting this expression into (42) we obtain

$$C_* = C^r(s(t),t) = C_{init} - f^b_0 erfc\frac{s_0}{\sqrt{D_r}}. \qquad (93)$$

This may be rearranged to obtain

$$f^b_0 = \frac{C_{init} - C_*}{erfc\left(\frac{s_0}{\sqrt{D_r}}\right)}. \qquad (94)$$

We note that in this model, the concentration in the glassy phase, C^g, is not continuous. Since there is no specific expression for $s'(t)$, clearly f^i_0 cannot be explicitly determined, and is therefore expressed in terms of s_0. We therefore need to establish bounds for f^i_0.

6) Conditions on f^i_0: The discontinuity is concentration at the front may be expressed as

$$[C]_{s(t)} = C^r(s(t)_+,t) - C^g(s(t)_-,t) \qquad (95)$$

which on substituting (93) and (61) is equivalent to

$$[C]_{s(t)} = C_{init} - f^b_0 \text{erf } c\left(\frac{s_0}{\sqrt{D_r}}\right) - $$
$$C_{ext} - m(t)e^{2ks_0\sqrt{t}} - f^i_0 \text{erf}\left(\frac{s_0}{\sqrt{D_g}}\right). \qquad (96)$$

Also, the partial differentials for C^g and C^r with respect to x are respectively

$$C^g_x(s(t)_-,t) = kme^{2ks_0\sqrt{t}} + \frac{f^i_0}{\sqrt{D_g t\pi}} e^{\frac{-s_0^2}{D_g}} \qquad (97)$$

and

$$C_x^r(s(t),t) = \frac{f_0^b}{\sqrt{D_r t \pi}} e^{\dfrac{-s_0^2}{D_r}} . \qquad (98)$$

On substituting these expressions in (23) given by

$$s'(t)[C]_{s(t)} = [J]_{s(t)}$$
$$= D_g C_x^g(s(t)_-, t) - D_r C_x^r(s(t), t), \qquad (99)$$

the following expression is obtained

$$s_0 \left[\begin{array}{c} C_{init} - f_0^b erfc(\frac{s_0}{\sqrt{D_r}}) - C_{ext} \\ -m(t)e^{2ks_0\sqrt{t}} - f_0^i \operatorname{erf}(\frac{s_0}{\sqrt{D_g}}) \end{array} \right] =$$

$$D_g \left(\sqrt{t}kme^{2ks_0\sqrt{t}} + \frac{f_0^i e^{\dfrac{-s_0^2}{D_g}}}{\sqrt{D_g \pi}} \right) - \frac{D_r f_0^b e^{\dfrac{-s_0^2}{D_r}}}{\sqrt{D_r \pi}} . \quad (100)$$

This can be rearranged to give

$$f_0^b \left(s_0 \operatorname{erf} c(\frac{s_0}{\sqrt{D_r}}) - \frac{\sqrt{D_r} e^{\dfrac{-s_0^2}{D_r}}}{\sqrt{\pi}} \right)$$

$$+ D_g \sqrt{t}kme^{2ks_0\sqrt{t}}$$

$$+ f_0^i \left(\frac{\sqrt{D_g} e^{\dfrac{-s_0^2}{D_g}}}{\sqrt{\pi}} + s_0 \operatorname{erf}(\frac{s_0}{\sqrt{D_g}}) \right) =$$

$$s_0 \left[C_{init} - C_{ext} - m(t)e^{2ks_0\sqrt{t}} \right]. \qquad (101)$$

As

$$f_0^b = \frac{C_{init} - C_*}{erfc(\frac{s_0}{\sqrt{D_r}})}, \qquad (102)$$

we obtain

$$\frac{C_{init} - C_*}{\operatorname{erf} c(\frac{s_0}{\sqrt{D_r}})} \left[\begin{array}{c} \sqrt{\frac{D_r}{\pi}} e^{\dfrac{-s_0^2}{D_r}} \\ -s_0 erfc(\frac{s_0}{\sqrt{D_r}}) \end{array} \right] +$$

$$s_0(C_{init} - C_{ext} - m(t)e^{2ks_0\sqrt{t}})$$

$$= f_0^i \left\{ \sqrt{\frac{D_g}{\pi}} e^{\dfrac{-s_0^2}{D_g}} + s_0 \operatorname{erf}(\frac{s_0}{\sqrt{D_g}}) \right\} + D_g \sqrt{t}kme^{2ks_0\sqrt{t}}$$

$$(103)$$

which is equivalent to

$$\frac{\sqrt{D_r} e^{-\dfrac{s_0^2}{D_r}} (C_{init} - C_*)}{\operatorname{erf} c(\frac{s_0}{\sqrt{D_r}})}$$

$$- f_0^i \left\{ \begin{array}{c} \sqrt{D_g} e^{\dfrac{-s_0^2}{D_g}} \\ + s_0\sqrt{\pi} \operatorname{erf}(\frac{s_0}{\sqrt{D_g}}) \end{array} \right\}$$

$$- s_0\sqrt{\pi}(C_{ext} + m(t)e^{2ks_0\sqrt{t}} - C_*)$$

$$- \sqrt{t\pi}D_g kme^{2ks_0\sqrt{t}} = 0. \qquad (104)$$

In this equation s_0 and f_0^i are the unknowns. f_0^i is a parameter that controls s_0, i.e., s_0 is a function of f_0^i. By varying s_0, the existence of solutions of (104) is shown and a bound is established for f_0^i.

Let

$$g(s_0) = \frac{\sqrt{D_r} e^{-\dfrac{s_0^2}{D_r}} (C_{init} - C_*)}{\operatorname{erf} c(\frac{s_0}{\sqrt{D_r}})}$$

$$- f_0^i \left\{ \sqrt{D_g} e^{\dfrac{-s_0^2}{D_g}} + s_0\sqrt{\pi} \operatorname{erf}(\frac{s_0}{\sqrt{D_g}}) \right\}$$

$$- s_0\sqrt{\pi}(C_{ext} + m(t)e^{2ks_0\sqrt{t}} - C_*)$$

$$- \sqrt{t\pi}D_g kme^{2ks_0\sqrt{t}} . \qquad (105)$$

For $s_0 = 0$, (105) becomes

$$g(0) = \sqrt{\frac{D_r}{D_g}}(C_{init} - C_*) - \sqrt{\pi t}\sqrt{D_g}km(t) - f_0^i. \quad (106)$$

If we assume that

$$f_0^i \leq \sqrt{\frac{D_r}{D_g}}(C_{init} - C_*) - \sqrt{\pi t}\sqrt{D_g}km(t),$$

and substitute this expression into (106), we obtain

$$g(0) > 0. \qquad (107)$$

We now proceed to analyse (105) for a different value of f_0^i and s_0.

$$\text{Let} \quad f_0^i \geqslant C_{init} - C_{ext} \text{ and } s_0 \to \infty. \qquad (108)$$

Substituting $s_0 \to \infty$ into (105), we have

$$- f_0^i s_0\sqrt{\pi} - s_0\sqrt{\pi}(C_{ext} + m(t)e^{2ks_0\sqrt{t}} - C_*)$$

$$- \sqrt{t\pi}D_g kme^{2ks_0\sqrt{t}} = \lim_{s_0 \to \infty} g(s_0), \qquad (109)$$

which may be rearranged as

$$-s_0\sqrt{\pi}(C_{ext} + m(t)e^{2ks_0\sqrt{t}} - C_*)$$
$$-\sqrt{t\pi}D_g kme^{2ks_0\sqrt{t}} - g(s_0) = f_0^i s_0\sqrt{\pi}. \qquad (110)$$

Substituting for f_0^i, we obtain

$$-s_0\sqrt{\pi}(C_{ext} + m(t)e^{2ks_0\sqrt{t}} - C_*)$$
$$-\sqrt{t\pi}D_g kme^{2ks_0\sqrt{t}} - g(s_0) \geqslant (C_{init} - C_{ext})\,s_0\sqrt{\pi}, \quad (111)$$

which gives

$$g(s_0) + \; s_0\sqrt{\pi}(C_{init} - C_* + m(t)e^{2ks_0\sqrt{t}})$$
$$+ \sqrt{t\pi}D_g km(t)e^{2ks_0\sqrt{t}} \leqslant 0. \qquad (112)$$

Since

$$\lim_{s_0\to\infty}\left[s_0\sqrt{\pi}(C_{init} - C_* + m(t)e^{2ks_0\sqrt{t}})\right] > 0 \qquad (113)$$

and

$$\lim_{s_0\to\infty}\left[\sqrt{t\pi}D_g km(t)e^{2ks_0\sqrt{t}}\right] > 0. \qquad (114)$$

We conclude that

$$g(+\infty) < 0. \qquad (115)$$

Using (107) ,(115) and assuming g(s_0) is continuous for all values of s_0, it follows that there is at least one value of s_0 that satisfies (104). This value occurs when

$$f_0^i \in \left[\begin{array}{c} C_{init} - C_{ext}, \sqrt{\frac{D_r}{D_g}}(C_{init} - C_*) \\ -\sqrt{\pi t}\sqrt{D_g}km(t) \end{array}\right], \qquad (116)$$

assuming that

$$C_{init} - C_{ext} \leqslant \left(\begin{array}{c} \sqrt{\frac{D_r}{D_g}}(C_{init} - C_*) \\ -\sqrt{\pi t D_g}km(t) \end{array}\right). \qquad (117)$$

Alternatively, given

$$f_0^i \geqslant \sqrt{\frac{D_r}{D_g}}(C_{init} - C_*) - \sqrt{\pi t D_g}km(t), \qquad (118)$$

and substituting this expression into (106), it follows that

$$g(0) < 0. \qquad (119)$$

Furthermore

$$f_0^i \geqslant C_{init} - C_{ext} \;\; \text{and} \; s_0 \to \infty, \qquad (120)$$

and substituting in (105) we see that,

$$g(\infty) > 0. \qquad (121)$$

Hence when

$$f_0^i \in \left[\begin{array}{c} \sqrt{\frac{D_r}{D_g}}(C_{init} - C_*) - \\ \sqrt{\pi t D_g}km(t), C_{init} - C_{ext} \end{array}\right] \qquad (122)$$

such that

$$C_{init} - C_{ext} \geqslant \left(\begin{array}{c} \sqrt{\frac{D_r}{D_g}}(C_{init} - C_*) \\ -\sqrt{\pi t D_g}km(t) \end{array}\right), \qquad (123)$$

and when we assume that $g(s_0)$ is continuous for all values of s_0, we may conclude that there is at least one value of s_0 that satisfies (104)

Hence for

$$f_0^i \in \left[\begin{array}{c} \min\left(\begin{array}{c} C_{init} - C_{ext}, \\ \sqrt{\frac{D_r}{D_g}}(C_{init} - C_*) - \sqrt{\pi t D_g}km(t) \end{array}\right), \\ \max\left(\begin{array}{c} C_{init} - C_{ext}, \\ \sqrt{\frac{D_r}{D_g}}(C_{init} - C_*) - \sqrt{\pi t D_g}km(t) \end{array}\right) \end{array}\right], \qquad (124)$$

(104) always has a solution. This gives us the bounds for f_0^i.

7) Large time behavior $t \to \infty$: From (70) we see that

$$f_\infty^b = \frac{C_{init} - C_*}{s_\infty\,\text{erf}\,c(\frac{s_0}{\sqrt{D_r}})}, \qquad (125)$$

which coincides with the previous result for small-times f_0^b (94). Thus, the equations for both C^g and C^r are equal in the small and large time limits, and s_∞ satisfies (105) when

$$f_0^b \equiv f_\infty^b \;\text{and}\; f_0^i \equiv f_\infty^i. \qquad (126)$$

We see that equation (105) has a solution $s_\infty = s_0$, which is represented by $\bar{s}$. Since there is no specified expression for the speed of the front, f^i cannot be determined and (124) gives the bounds of f^i. Hence s appears as a function of f^i.

VI. NUMERICAL METHOD

Let $x_j = x_{j-1} + h$, $j = 1, \ldots, N-1$, $x_0 = 0$, $x_N = L$, be the spatial grid in $[0, L]$ for a sufficiently large sample size L. For the interval $[0, T]$, $T > 0$ we consider the time grid t_j, $j = 0, \ldots, M$, $t_0 = 0$, $t_j - t_{j-1} = \Delta t$, $j = 1, \ldots, M$. At each point in time t_n, $s(t_n) \simeq s_n$ is the corresponding spatial point, that is $s_n = x_{i_n^*}$ for some $i_n^* \in \{1, \ldots, N\}$. We utilize $C_h^{n+1} = (C_{h,g}^{n+1}, C_{h,r}^{n+1})$ with $C_{h,g}^{n+1} = (C_{j,g}^{n+1}, j = 1, \ldots, s_{n+1}), C_{h,r}^{n+1} = (C_{j,r}^{n+1}, j = s_{n+1}, \ldots, N-1)$ to represent the discrete approximations of C^g and C^r thereby defined as

$$C_{h,g}^{n+1} = C_{h,g}^n + \Delta t D_g D_{2,x} C_{h,g}^{n+1},$$
$$\qquad\qquad\qquad\qquad\qquad (127)$$
$$C_{h,r}^{n+1} = C_{h,r}^n + \Delta t D_r D_{2,x} C_{h,r}^{n+1}.$$

We use the same notation as (127) where $D_{2,x}$ denotes the second-order finite-difference operator. A moving grid criterion is included in the finite difference scheme. This is

obtained by an explicit discretization of the front equation (23) as

$$s_{n+1} = s_n + \Delta t \frac{[J]_{s_n}}{[C]_{s_n} + \gamma}, \qquad (128)$$

where γ is an arbitrarily small positive constant, and

$$[J]_{s_n} = -D_r D_{-x} C^n_{i^*_n+1} + D_g D_{-x} C^n_{i^*_n},$$

$$[C]_{s_n} = C_* - C^n_{i^*_n-1}.$$

Here, the backward finite-difference operator is denoted by D_{-x}.

As $s_{n+1} \in [x_\ell, x_{\ell+1}]$ for some given ℓ, the transition point $x_{i^*_{n+1}}$ is defined as

$$x_{i^*_{n+1}} = x_\ell \text{ if } s_{n+1} \leq (x_\ell + x_{\ell+1})/2 \,, \text{ else } x_{i^*_{n+1}} = x_{\ell+1}. \qquad (129)$$

Equations (127) and (128) are complemented by the discrete boundary conditions

$$D_{+x} C^{n+1}_{0,g} = k(C^{n+1}_{0,g} - C_{ext}),\ C^{n+1}_{i^*_{n+1},r}$$

$$= C^\star,\ D_{-x} C^{n+1}_{N,r} = 0 \qquad (130)$$

where the initial condition is represented as

$$C^0_j = C_{init}\,. \qquad (131)$$

As previously discussed, we do not have an explicit expression for the front velocity to the facilitate the numerical computation of $C^{n+1}_{h,g}$ defined in (127). We therefore replace the implicit equation

$$C^{n+1}_{i^*_{n+1}-1} = C^n_{i^*_{n+1}-1} + \Delta t D_g D_{2,x} C^{n+1}_{i^*_{n+1}-1} \qquad (132)$$

with an explicit formulation. In this case we consider $C^g(s(t_{n+1})_-) \simeq \sum_{i<i^*_{n+1}} \alpha_i C^{n+1}_i$, with $\alpha_i \in [0,1]$ and $\sum_i \alpha_i = 1$.

VII. NUMERICAL RESULTS

Several numerical calculations were carried out. In this paper we present our numerical results for the following parameters:

$$C* = 0.7,\ D_r = 1.0,\ D_g = 0.4,\ L = 4,$$

$$C_{ext} = 0.3,\ \Delta t = 1 * 10^{-4}, h = 0.027 \qquad (133)$$

In Figure 1, we show a graph of the concentration for various times. The general shape of the concentration curves is similar to the experimentally obtained desorption curve   s shown in [1]. As expected, there is a distinct change in gradient of these curves after the critical concentration C_* has been crossed. By varying the magnitude of C_*, the exact position of the transition to the glassy state may be altered. The ratio $\frac{D_g}{D_r}$ may also be modified to regulate the transition from the saturated rubbery state to the dry glassy configuration.

During the desorption process, another phenomenon (besides literal skinning) called trapping skinning, can occur. In trapping skinning, an increase in the force driving the desorption – by decreasing the external concentration or increasing the permeability of the exposed end [20] – will actually decrease the accumulated flux through the boundary. It should be noted that the lower diffusion coeffcient in the glassy skin (from literal skinning) is not adequate to describe such behavior.

We now consider the trapping skinning effect. As explained by Edwards [14], the driving force for desorption can be enhanced by decreasing the external concentration C_{ext} or by increasing k – the permeability of the exposed end. The trapping skinning effect causes an increase in the driving force to decrease the accumulated flux for small times.

We set $C_{ext} = 0.0$, increase this to $C_{ext} = 0.1$ and then to $C_{ext} = 0.4$. The numerically calculated values of the accumulated flux are then plotted against time. Figure 2 shows that although the driving force and accumulated flux are greatest when $C_{ext} = 0.0$, this graph is similar to the graph for $C_{ext} = 0.1$, and the graphs can be superimposed for small times.

Figure 3 shows the graphs of accumulated flux against time for $k = 100, 300$ and 600. On comparison of the graphs, it is observed that although the driving force and accumulated flux are smallest when $k = 100$, there is not much change in the graphs when k and hence the driving force is increased for $k = 300$ and $k = 600$. In fact, these two graphs are almost superimposed for $t > 1$

It should be noted that the scaling of the parameters is based on pure intuition, as no experimental data is available for direct testing of the model. Added to this, restrictions on numerical stability of the scheme prevents extensive testing with widely varying parameters. Although these may seem to be enormous limitations, and a discredit to our model, as we base our model on tested and experimentally verified equations governing diffusion in polymers, we are confident that our model can act as a stepping stone towards a more comprehensive study of desoprtion. We wish to remind the reader that to the best of our knowledge, no experimentalists have developed suitable equipment to measure the speed of the desorption front. Indeed, this would be essential for the proper validation of our model. However, such experimental verification is both beyond the scope of this present study and the capability of polymer experimentalists to-date.

VIII. DISCUSSION OF NUMERICAL RESULTS

Trapping skinning is akin to anomalous diffusion in the sense that both represent unusual diffusion phenomena. An increase in the force driving desorption should naturally reflect an increase in the accumulated flux. However, in trapping skinning the reverse occurs, and an increase in the driving force results in a decrease in the accumulated flux. This is thus contrary to expectations and cannot be explained solely by the lower diffusion coefficient of the encapsulating glassy skin formed due to literal skinning.

According to our analysis, under certain conditions, as C_{ext} increased – and hence the driving force for desorption decreased – the accumulated flux increased. Figure 1 shows that the graphs of $C_{ext} = 0.0$ and $C_{ext} = 0.1$ can be superimposed for small times. A decrease in the external concentration and
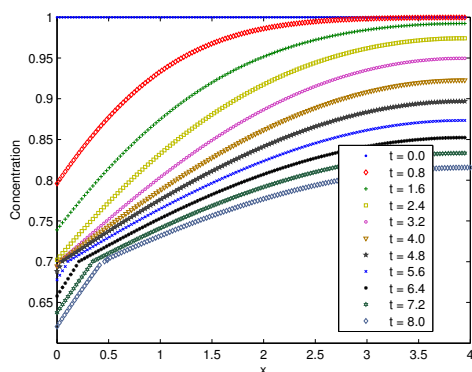
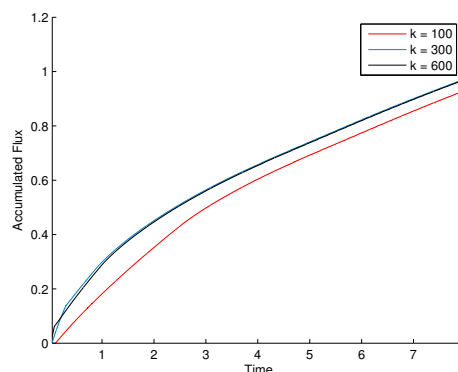Fig. 1.   Concentration profiles at various times

Fig. 3.   Illustration of the trapping skinning effect: Varying the permeability constant
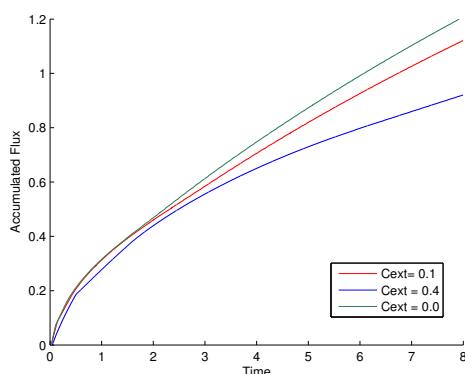

Fig. 2.   Illustration of the trapping skinning effect: Varying the external concentration

hence an increase in the driving force had little effect on the accumulated flux thus illustrating the trapping skinning effect.

In addition, trapping skinning also appeared when we considered the behavior of k [14]. Edwards noted that an increase in k – the permeability of the exposed boundary – would increase the driving force. According to Figure 3, an increase in k – and hence the driving force – from 300 to 600 resulted in little change in the accumulated flux. However, the trapping skinning effect was not deduced when $k = 100$. There also appeared to be less of an effect when we considered changes in the driving force due to k as opposed to C_{ext}. We note that a thorough investigation into these observations cannot be accomplished without adequate experimental support, and to the authors' knowledge, such empirical evidence is not currently available.

We wish to make it clear that at the current stage of development, the polymer desorption model outlined does not attempt to offer any explanation of the physical mechanisms underlying the trapping skinning effect. However it is notable that the general shape of our numerically determined polymer desorption curves are similar to those obtained from experimental data [1], [16], [22], [23]. The method employed to obtain an expression for front speed serves our purpose,

at least until experimentalists manage to obtain an analytical expression for the speed of the desorption front.

IX. CONCLUSION

The phenomenological model considered was an extension of one by Comissiong *et al* [17], in which a more practical boundary condition - a radiation condition - was applied to the exposed end. The ensuing model consisted of a pair of coupled partial differential equations with a moving, approximately Fickian front separating the glassy and rubbery regions. Since this system was not solvable by similarity solutions, an integral method was used to obtain asymptotic solutions. Since the expression for the front speed is given in terms of a parameter, the model can also be adapted easily should the experimentalists come up with an analytical expression or value.

One of the basic assumptions used in the model was the treatment of the polymer as a one dimensional object. Though this assumption was justified in [24], by neglecting changes in the size of the polymer as it is being desorbed, this assumption appeared intuitively unrealistic. However, according to Samus and Rossi [1], this one dimensional approach may be deemed appropriate as most of the experimental work undertaken on diffusion in polymers used either films or samples in which the thickness was significantly smaller than the length or the width.

Assumptions were also made about the behavior of the diffusion coefficient. There was a critical transition concentration C_* at which the polymer changed state from rubbery to glassy, and this was built into the definition of $D(C)$. The difference within states were assumed negligible when compared with difference between states. According to Hui and Wu [19], these assumptions are all consistent with experimental observations. Hence we are justified by taking $D(C)$ to be an average over each polymer phase. Sanopoulou and Petropoulos (1999) observed, on studying desorption processes, a close similarity in shape between Fickian and non-Fickian desorption curves. Thomas and Windle in [10] also remarked that the process of penetrant desorption from a plasticised rubber is

expected to have Fickian characteristics. Hence the governing equation for the position of the front we used was a Fickian one $s(t) = 2s_0\sqrt{t}$.

In the analysis for small times, it was noted that if continuity was imposed to the concentration, then for $n > \frac{1}{2}$, $C_\star = C_{ext}$. This was of course not possible for desorption. Hence the concentration was found to be discontinuous at the front which was one of the model assumptions. We claim that this lack of continuity contributes to give the front a certain non-Fickian character. Based on experimental results, Samus and Rossi [1] described the "existence of two regimes for desorption: an initial fast regime followed by a very slow desorption regime whose onset depends on the temperature of the experiment". According to Bagley and Long [23],
"The sorption and desorption for this rapid initial stage follow Fick's law ...The second, slow stage of sorption and desorption does not obey Ficks law". Hence our expression for front speed appears reasonable until experimentalists can agree upon an analytical expression for the speed of the front.

While the model illustrates the rough characteristics of the trapping skinning effect, there was no provision in the formulation to account for for the encapsulating glassy skin that has been observed experimentally (almost instantaneously) at the start of the desorption process. This skin should slow down the process of desorption. This is the subject of ongoing work, and is briefly outlined here.

Two boundary layers may be introduced into the model – one inserted near the exposed end, $x = 0$ and the other (which may be either an interior or corner layer) placed near the moving boundary $x = s(t)$. The definitions of concentration at the front and the boundary conditions remain the same and will assist in the matching process. The boundary Layer at $x = 0$ may be found as follows. Let the thickness of the initial glassy skin be η. (This can be found experimentally). It is also assumed that $0 < \epsilon << 1$. According to [25], the diffusion coeffcient in the glassy skin is much lower than in the rubbery region and can be written as $D^{gg} = D_0\epsilon$, where D_0 is a constant [15].

The problem at $x = 0$ is reduced to solving $C_t^g(0,t) = D_0\epsilon C_{xx}^g(0,t)$ subject to $C^g(0,t) = C_{ext}$ where $t \geqslant 0$, (so there is always a glassy skin of thickness η), and the radiation condition is applied at $x = \eta$ i.e. $C^g(\eta,t) = C_{ext} + m(t)e^{kx}$. Using matched asymtotic expansions, we may assume that there is a boundary layer at $x = 0$, $C^{gg}(\zeta,t) = C^g(0,t)$, and $\lim_{\zeta\to\infty} C^{gg}(\zeta,t) = \lim_{x\to o} C^g(0,t) = C_{ext}$ where $\zeta = \frac{x}{\epsilon^\alpha}$ and α is a constant to be determined. The moving boundary layer at $x = s(t)$ may be either an interior or a corner layer. However due to the discontinuous conditions imposed at the front, an inner layer can be assumed to exist at $s(t)$. Since the concentration at the front is discontinuous, we have to match the solutions of $C^r[s(t),t] = C_\star$ and $C^g[s(t),t]$. The problem at $x = s(t)$ can therefore be reduced to solving $C_t^g(x,t) = D_1\epsilon C_{xx}^g(x,t)$ in the domain $0 \leqslant x \leqslant s(t)$ with a boundary layer near $s(t)$, where $C^g(\eta,t) = C_{ext} + m(t)e^{kx}$ and $C^g(s(t),t) = C_\star$.

We conclude by saying that our model hints at but did not examine the possibility of boundary layers in the model. This naturally led to recommendations for yet a further evolution of the Comissiong *et al.* model using asymptotic techniques to examine the existence and type of these boundary layers. Though this model appears amenable to changes, with more research being done in polymer diffusion, the real test will be how well the model stands up to experimental data, when it becomes available.

REFERENCES

[1] M. A. Samus and G. Rossi. Methanol absorption in ethylene-vinyl achohol copolymers: Relation between solvent diffusion and changes in glass transition temperature in glassy polymeric materials. *Macromolecules*, 29(6):2275–2288, 1996.

[2] G. Astarita and S. Joshi. Simple dimension effect in the sorption of solvents in polymer – a mathematical model. *J. Membr. Sci.*, 4:165–182, 1978.

[3] G. Astarita and G. C. Sarti. A class of mathematical models for the sorption of swelling solvent in glassy polymers. *Polym. Eng. Sci.*, 18:388–397, 1978.

[4] A. Friedman and G. Rossi. Phenomenological continuum equations to describe case ii diffusion in polymeric materials. *Macromolecules*, 30:153–154, 1997.

[5] A. Peterlin. Diffusion in a network with discontinuous swelling. *J. Poly. Sci. B: Polym. Lett.*, 3:1083–1092, 1965.

[6] T. Qian and P. L. Taylor. From the thomas windle model to a phenomenological description of case ii diffusion in polymers. *Polymer*, 52(19):7159–7163, 2000.

[7] G. Rossi, P. A. Pincus, and P. G. De Gennes. A phenomenological description of case ii diffusion in polymeric materials. *Europhys. Lett.*, 32:391–396, 1995.

[8] N. L. Thomas and A. H. Windle. Transport of methanol in poly(methylmethocrylate). *Polymer*, 19:255–265, 1978.

[9] N. L. Thomas and A. H. Windle. A deformation model for case ii diffusion. *Polymer*, 21:613–619, 1980.

[10] N. L. Thomas and A. H. Windle. Diffusion mechanics of the system pmma-methanol. *Polymer*, 22:627–639, 1981.

[11] N. L. Thomas and A. H. Windle. A theory of case ii diffusion. *Polymer*, 23:529–542, 1982.

[12] R. W. Cox and D. S. Cohen. A mathematical model for stress driven diffusion in polymers. *J. Poly. Sci. B: Poly. Phys.*, 27(3):589–602, 1989.

[13] D. A. Edwards. A spatially nonlocal model for polymer-penetrant diffusion. *J. Appl. Math. Phys.*, 52:254–288, 2001.

[14] D. A. Edwards. A mathematical mode for trapping skinning in polymers. *Stud. Appl. Math.*, 99:49–80, 1997.

[15] D. A. Edwards and R. A. Cairncross. Desorption overshoot in polymer-penetrant systems: Asymptotic and computational results. *SIAM J. Appl. Math.*, 63:98–115, 2002.

[16] M. Sanapoulou, D. F. Stamatialis, and J. H. Petropoulos. Investigation of case ii behavior. 1. theoretical studies based on the relaxation dependent solubility model. *Macromolecules*, 35(3):1012–1020, 2002.

[17] D. M. G. Comissiong, J. A. Ferreira, and P. de Oliveira. A phenomenological model for desorption in polymers. University of Coimbra,CMUC Technical Report 06-35, 2006.

[18] M. Sanopoulou and J. H. Petropoulos. Systematic analysis and model interpretation of micromolecular non-fickian sorption kinetics in polymer films. *Macromolecules*, 34:1400–1410, 2001.

[19] C.Y. Hui, R. C. Wu, R. C. Lasky, and E. J. Kramer. Case ii diffusion in polymers. ii. steady state front motion. *J. Appl. Phys.*, 61:5137–5149, 1987.

[20] D. A. Edwards. Skinning during desorption of polymers: An asymptotic analysis. *SIAM J. Appl. Math.*, 59:1134–1155, 1999.

[21] J. Crank. *The Mathematics of Diffusion*. Oxford University Press, Oxford, U.K., 1973.

[22] J. Crank. A theoretical investigation of the influence of molecular relaxation and internal stress. *J. Poly. Sci.*, 11:151–168, 1953.

[23] E. Bagley and F. A. Long. 2-stage sorption and desorption of organic vapours in cellulose acetate. *J. Am. Chem. Soc.*, 77:2172–2178, 1955.

[24] D. A. Edwards. An asymptotic analysis of polymer desorption and skinning. *Macromolecular Theory and Simulations*, 8:10–14, 1999.

[25] G. Powers and J. Collier. Experimental modeling of solvent-casting thin polymer films. *J. Poly. Eng. Sci.*, 30:118–123, 1990.